Journal of

Applied and Computational Mechanics

Shahid Chamran
University of Ahvaz

Investigation of Wood Properties at Elevated Temperature

Anatoly M. Bragov[1], Tatyana N. Iuzhina[2], Andrei K. Lomunov[3], Leonid A. Igumnov[4], Aleksandr A. Belov[5], Victor A. Eremeyev[6,7]

[1] National Research Lobachevsky State University of Nizhny Novgorod, Gagarin ave. 23, Nizhny Novgorod, 603950, Russian Federation, Email: bragov@mech.unn.ru

[2] National Research Lobachevsky State University of Nizhny Novgorod, Gagarin ave. 23, Nizhny Novgorod, 603950, Russian Federation, Email: yuzhina_tatiana@mech.unn.ru

[3] National Research Lobachevsky State University of Nizhny Novgorod, Gagarin ave. 23, Nizhny Novgorod, 603950, Russian Federation, Email: lomunov@mech.unn.ru

[4] National Research Lobachevsky State University of Nizhny Novgorod, Gagarin ave. 23, Nizhny Novgorod, 603950, Russian Federation, Email: igumnov@mech.unn.ru

[5] National Research Lobachevsky State University of Nizhny Novgorod, Gagarin ave. 23, Nizhny Novgorod, 603950, Russian Federation, Email: belov_a2@mech.unn.ru

[6] Department of Mechanics of Materials and Structures, Faculty of Civil and Environmental Engineering, Gdansk University of Technology,
11/12 Gabriela Narutowicza Street, Gdansk, 80-233, Poland, Email: eremeyev.victor@gmail.com

[7] Department of Civil and Environmental Engineering and Architecture (DICAAR), University of Cagliari, Via Marengo, 2, 09123 Cagliari, Italy, Email: victor.eremeev@unica.it

Abstract. The results of dynamic compression tests of aspen under elevated temperature up to +60°C are presented. The tests were carried out based on the Kolsky method using the split Hopkinson pressure bar. To study the anisotropy of properties, aspen samples were fabricated and tested by cutting along and across the fibers direction. Dynamic stress-strain curves were obtained as well as the average values of modulus of active loading sites. The greatest steepness of the loading branches and the highest breaking stresses are observed for the samples loaded along the fiber direction, while the smallest values are noted under loading across the fiber direction. Also the effect of elevated temperature on strength and deformation properties of aspen is estimated.

1. Introduction

For transportation and storage of spent nuclear fuel and other high level waste, transport packages are used. They are equipped with damping shock absorbers to reduce dynamic loads on the body and protect its contents from damage as a result of careless handling, including emergency operating conditions [1, 2]. The damping material for transport package set must satisfy the following requirements: high ability to absorb and dissipate impact energy; it should have low density, since the mass of the damping device and, as a consequence, the mass of the entire transport package set depend on it; material availability; the possibility of machining; minimum cost; environmental friendliness.

Different wood species, fiber-expanded clay concrete and synthetic foams are proposed as damping material along with aluminum or copper. When choosing damping material, one of the criteria for comparative evaluation is specific indicators. They are determined by the ratio of the mechanical characteristic (tensile strength, elastic modulus, impact strength, hardness) to the density of the material. Specific characteristics are of particular importance when the design requires high strength and ability to absorb impact at low weight.

In terms of specific strength, wood is quite competitive with other modern materials. In addition, wood materials have a high ability to absorb impact energy. Under prolonged loads, the wood behaves as a compliant body, the deformations of which are large. Under short-term impact, wood exhibits the properties of a relatively rigid, slightly deformable body. Having low density, wood is well machined, available and relatively low-cost material. In Germany, a welded steel sheet construction filled with wood is common for impact energy absorber. The wood is the main energy absorber and the steel sheet ensures the integrity of the impact limiter.

The models of wood deformation and failure are being developed actively throughout the world. They can be used in various calculation complexes for modeling the behavior of technically complex structures containing elements of wood [3, 4, 5, 6, 7]. The fundamental model for wood has been studied for many years and a significant progress has been made. New models can also take into account temperature and strain rate, and in most cases are able to meet the requirements for calculations of structures made of wood. However, due to complexity of the wood neither of models can be used for all purposes. Thus, in order to solve technically complex problems it is necessary to use different models.
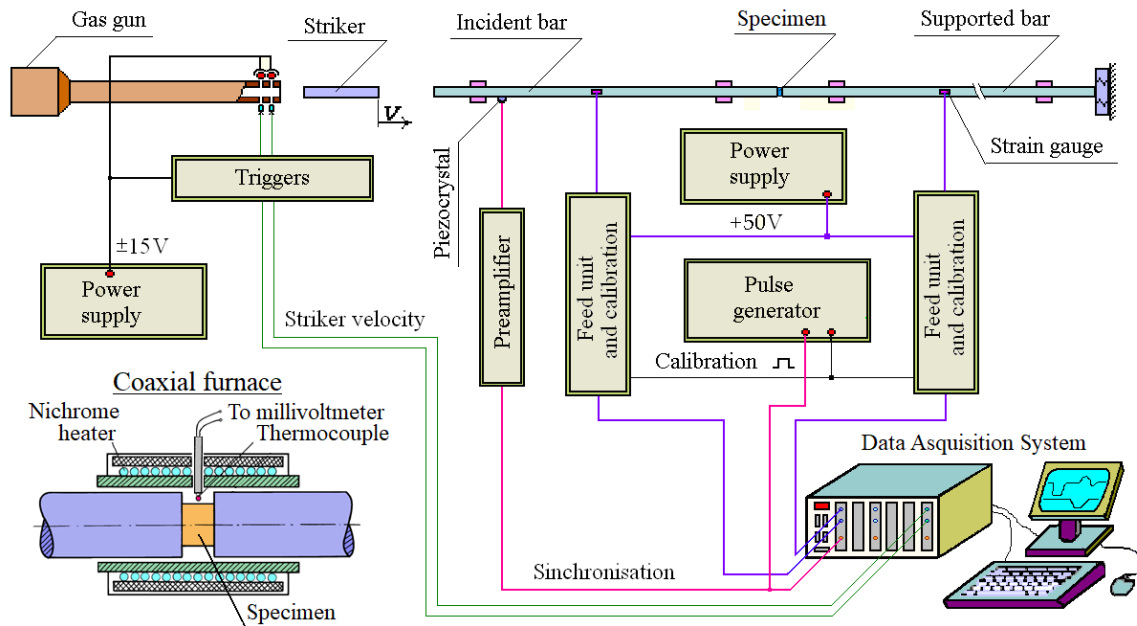
Fig. 1. Experimental setup

Wood exhibits significant anisotropic deformation behavior under elastic and plastic compression. This is almost due to its cellular microstructure. Cells are aligned along their long axis in the direction of the trunk. Therefore, the deformation behavior along the long cell axis (longitudinal) is different from that of cells perpendicular to this direction. Moreover, the difference in behavior between radial and tangential deformation is relatively small. Wood can be described as elastoplastic, transverse-isotropic, cellular material. The behavior of wood under load can be divided into three types: elasticity, ductility and compaction. Sometimes compaction does not seem to be very important, but it cannot be ignored in mechanical analysis, in general.

Earlier in [8], the aspen properties at room temperature were investigated. However, since containers are transported in different climatic conditions, there is an urgent need to study the properties of wood at elevated temperatures up to +50 ÷ +60°C.

In the present work, we studied the behavior of aspen samples with longitudinal and transverse cutting of samples at a temperature of +60°C under dynamic compression.

2. Experimental Technique

To conduct dynamic tests of aspen samples at elevated temperatures, an experimental setup [9] was used that implements the Kolsky method using a split Hopkinson pressure bar (SHPB). The setup includes a loading device (gas gun), a set of measuring bars and recording equipment. The installation diagram is shown in Fig. 1. Measuring bars with a diameter of 20 *mm* are made of aluminum alloy D16T. Using small-base strain gages glued to the lateral surface of the measuring bars, we record elastic strain pulses: incident $\varepsilon_i(t)$, reflected $\varepsilon_r(t)$ and transmitted $\varepsilon_t(t)$. On their basis, using the formulas of the Kolsky method [10], the parametric dependences of sample stress, strain and strain rate development over time are determined. After synchronization of these pulses, the curves $\sigma_s(\varepsilon_s)$ and $\dot{\varepsilon}_s(\varepsilon_s)$ are constructed.

These pulses are measured by low-base strain gauges made of thin constantan foil and glued to the side surface of the measuring bars. To compensate for bending vibrations in the bars and increase the amplitude of the output signal in the working sections, four strain gages are glued, connected in series. For undistorted registration of pulses of maximum duration, in the bars, working strain gauges are glued approximately in the middle of the bar length at the same distance from the sample. Since during the test only the dynamic strain component in the bar is recorded, a potentiometric circuit was chosen to power the strain gages due to its simplicity and the possibility of supplying several measuring channels from one source. Both groups of strain gages are supplied with direct current from one standard stabilized power supply. To register signals from strain gauges and from a striker velocity meter, a multichannel computer measuring system PXI-1042 from National Instruments is used. To start the recording equipment, a piezoelectric crystal is used, fixed on the lateral surface of the input bar, near the impact end. The signal from it is fed through the preamplifier to the input of the external trigger of the oscilloscope. For the conversion from the values of the electrical signal to the values of deformations in the bars, the measuring channels are calibrated, and to improve the accuracy of the results, the calibration is performed before each series of tests. The electrical diagram of the original strain gauge feed and calibration unit is shown in Fig. 2.

The calibration system includes a two-channel quartz-type rectangular pulse generator, small-sized reed relays K1 and calibrated scale resistors R6 (Fig. 2). When the relay is triggered, scale calibrated resistors R6 are connected to the R7 strain gauges, which simulates a jump-like change in the resistance of the strain gauges. This causes a proportional jump in the line on the oscilloscope screen. By measuring the value a of the deflection of the beam on the oscilloscope screen when the resistance of the strain gauge R=R7 changes by a known value ΔR=R6 during calibration, it is easy to calculate the calibration coefficient K^Y, which connects the value of the deflection of the beam a obtained on the screen during testing and the corresponding amplitude of deformation pulses in the bars $K^Y=\Delta R/(R*k*a)$, where k is the strain gage coefficient.

Since the length of the loading pulse is much greater than the length of the sample, it undergoes compression under uniaxial and uniform stress conditions, i.e. the deformation process is similar to the quasistatic one that occurs only at high strain rate (about 10^3s^{-1}).
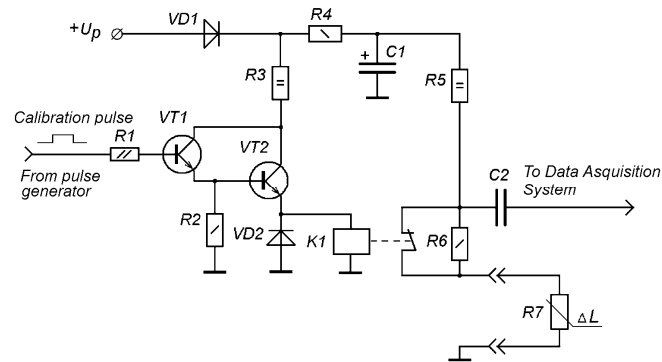
Fig. 2. Electrical scheme of feed unit and calibration

To register elastic deformation pulses in the measuring bars, a high-precision measuring system from National Instruments is used. Processing of the primary experimental data, including synchronization of initial pulses and their smoothing, as well as construction of deformation diagram $\sigma_s(\varepsilon_s)$ with the strain rate dependence $\dot{\varepsilon}_s(\varepsilon_s)$ is carried out using the original program.

In the present work, we studied the behavior of aspen samples with longitudinal and transverse cutting of samples at a temperature of +60°C under dynamic compression.

A miniature tube-shaped furnace was used to heat the test samples to +60°C (as shown in Fig. 1). It is located on the ends of the measuring bars with a sample placed between them. The furnace is a tube 150 *mm* long with an inner diameter of 22 *mm*. A layer of nichrome wire was wound around the tube, insulated from the outside with a layer of mica, asbestos and fiberglass. A small hole was left in the middle of the furnace length for passing thermocouple inside the furnace to the side sample surface for temperature control. During the working day, the ends of the measuring bars in the working area were kept constantly in a heated state. This eliminated the temperature loss by the sample when it was placed in the working position. Since this temperature was much lower than half of the melting temperature of the bar, at which noticeable changes in elastic characteristics of the bar (elastic wave velocity and elastic modulus) occur. Neither formulas nor processing method of experimental data were corrected.

The test procedure was as follows:
– the furnace was put on the ends of the measuring bars, connected to an adjustable voltage source and it was heated to a temperature of ~60°C (thermocouple control) for at least 30-50 *min*; thus, the ends of the measuring bars were constantly in the heated state during the tests that excluded the sample from losing temperature when it was placed between the bar ends;
– all available samples of a given batch were measured (wood species and cutting angle), weighed and initial sample density was determined;
– since wood has very poor thermal conductivity, the samples were placed in a heating chamber with a temperature of + 60℃ before testing, where they were kept for at least an hour; to reduce drying, the samples were located in a chamber in a metal box;
– an experimental setup was being prepared for testing, the furnace was shifted along one of the measuring bars, releasing the gap between their ends, the sample was removed from the heating chamber, quickly enough (10-15 *s*) was placed in the working position, and the furnace was moving on it;
– after a short (1-2 *min*) exposure of the sample in the furnace cavity, a test was carried out, the sample was removed from the furnace and, if its integrity was preserved, it was measured quite quickly (less than 1 minute), installed in the working position and kept for 2-3 *min* and loaded again.

3. Test Samples

For compression testing of aspen with air humidity (~12%) at elevated temperature, samples were made in the form of cylinders with a height of ~10 *mm* and a diameter of ~20 *mm* with different cutting direction relative to the fibers orientation. The angles between the direction of applied load and that of fiber arrangement were 0° and 90°. The flat ends of the samples before testing were carefully sanded.

4. Test Results

A set of tests on aspen samples cut along and across the fibers at a temperature of +60°C has been carried out. The experiments aimed at determining the ultimate stress leading to visible discontinuities, cracks, and chips a in the sample. For this, the samples were loaded with different strain rates determined by the impactor velocity. Some samples that retained their apparent integrity after one loading cycle were loaded a second time (and some even a third time) with increasing each time loading wave amplitude.

The main premise of the Kolsky method is the uniformity of the stress-strain state of the sample during the test. This condition is checked by comparing the strain pulses at two ends of the sample $\varepsilon^i(t) + \varepsilon^r(t) = \varepsilon^t(t)$ during the entire test. Figure 3 shows the strain pulses in the measuring bars: incident $\varepsilon^i(t)$, reflected $\varepsilon^r(t)$, transmitted $\varepsilon^t(t)$. The red dotted line shows the total momentum $\varepsilon^i(t) + \varepsilon^r(t)$. One can see a good agreement between the strain pulses at both ends of the sample during the entire loading.

The following feature of the wood sample behavior under dynamic loading can be noted: it is clearly seen that the reflected and transmitted pulses do not return to the zero line after the loading process. The process of unloading has a very long duration due to the high viscosity of the material. Therefore, it is completely impossible to register the process of unloading due to the limited length of the measuring bars.

Table 1. Test conditions and results

Experience Number	The density of the sample (g/cm³)	Impactor length (mm)	Impactor speed (m/s)	Residual strain (%)	The module of the load branch (MPa)	Tensile strength (MPa)
Loading along the fibers						
312-07/1	0.496	300	11.4	2.70	2229	72.0
312-07/2	0.496	300	13.7	2.20	3074	81.6
312-07/3	0.496	300	20.0	8.50	3333	78.7
312-08/1	0.479	300	11.1	1.70	1512	56.5
312-08/2	0.479	300	13.5	2.50	2923	75.7
312-08/3	0.479	300	20.0	7.50	2961	84.2
312-09/1	0.478	300	15.9	5.00	2229	79.1
312-09/2	0.478	300	20.0	7.00	3071	86.2
312-10/1	0.489	300	20.0	7.40	2349	84.6
312-10/2	0.489	200	27.8	17.50	2210	74.5
312-11	0.484	200	28.1	25.80	2930	86.5
Loading across the fibers						
316-09/1	0.486	300	4.8	2.00	289	5.3
316-09/2	0.486	300	4.2	1.00	149	4.2
316-09/3	0.486	300	4.7	1.00	145	3.8
316-09/4	0.486	300	15.4	22.00	124	7.19
316-10/1	0.488	300	4.1	2.00	351	4.9
316-10/2	0.488	300	7.3	4.50	150	6.3
316-10/3	0.488	300	9.3	8.00	117	7.0
316-10/4	0.488	300	15.9	19.00	108	11.0
316-11	0.376	300	15.6	8.50	110	3.8
316-12	0.423	200	28.1	38.00	139	5.2

Table 1 shows the conditions for testing samples along and across fibers as well as some strength and strain characteristics. Each test is assigned an identification number consisting of a three-digit material code and after a hyphen a specific sample number in the test batch. In the process of testing, samples were subjected to both single loading to failure and repeated reloading, since the integrity of such samples after testing was more or less preserved. The diagrams of repeated loading are located on the strain axis conditionally: sequentially after the corresponding diagrams of the previous loading cycle.

Figures 4-7 show the obtained strain diagrams $\sigma_s(\varepsilon_s)$ and the corresponding dependences of the strain rate $\dot{\varepsilon}_s(\varepsilon_s)$ for the samples under loading along the fibers. The diagrams of repeated tests are located conditionally on the strain axis: each subsequent diagram begins with the deformation obtained by the sample in the previous load cycle.

Figure 4 shows diagrams of triple loading of sample 312-07 along the fibers with the impactor velocity increasing from experiment to experiment, but with rather close values of the strain rate while maintaining the integrity of the sample (curves 312-07/1 and 312-07/2) and slight destruction of the sample (curve 312-07/3). After the first two loading cycles, the sample retained its integrity, although it acquired a residual deformation of about 2%. In the third cycle, the residual strain was 8.5%, the sample received a uniform radial distribution and minor longitudinal cracks were formed on its lateral surface.

In the lower part of the figure, the dashed lines indicate corresponding dependences of the strain rate change $\dot{\varepsilon}_s(\varepsilon_s)$. It can be seen that, in the absence of sample failure (first cycle), the strain rate decreases steadily after reaching its maximum, whereas during the failure of the sample (third cycle), the strain rate increases in the area of active loading. Then it begins to decrease, but after the sample reaches the stress peak and beginning of the relaxation zone, the strain rate is observed to increase again.

The loading branches of the diagrams $\sigma_s(\varepsilon_s)$ are nonlinear, especially in the initial part, the unloading branches are closer to linear ones and have a greater steepness. As can be seen from the curves obtained, the strength of the sample at a strain rate of $\sim 800\,s^{-1}$ was about $75\,MPa$. When this level is exceeded, a stress relaxation region with increasing strain degree is observed which testifies to failure. Nevertheless, elastic unloading of the sample occurs after the end of the loading pulse.

A behavior feature of aspen during cyclic loading along the fibers is a slight increase in the deformation modulus $d\sigma/d\varepsilon$ (steepness of the active loading section), i.e. material after previous loading becomes more rigid. The dashed lines show the linear approximations of the sections of active loading with the corresponding equations. In the third loading cycle, the deformation modulus increased by a factor of 1.5 compared with the one in the first cycle. Certain values of the modules of the loading branches of the diagrams are listed in Table 1.
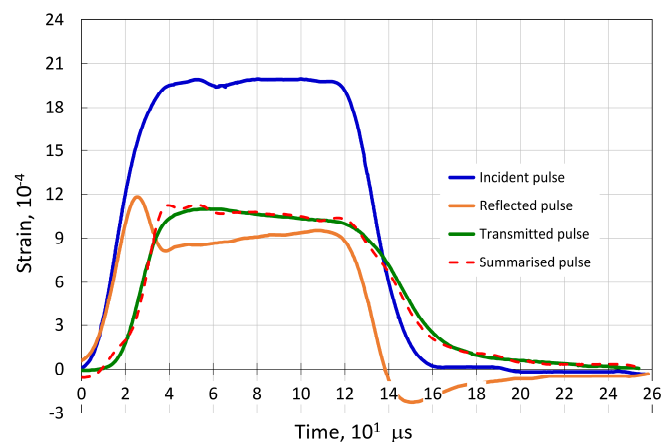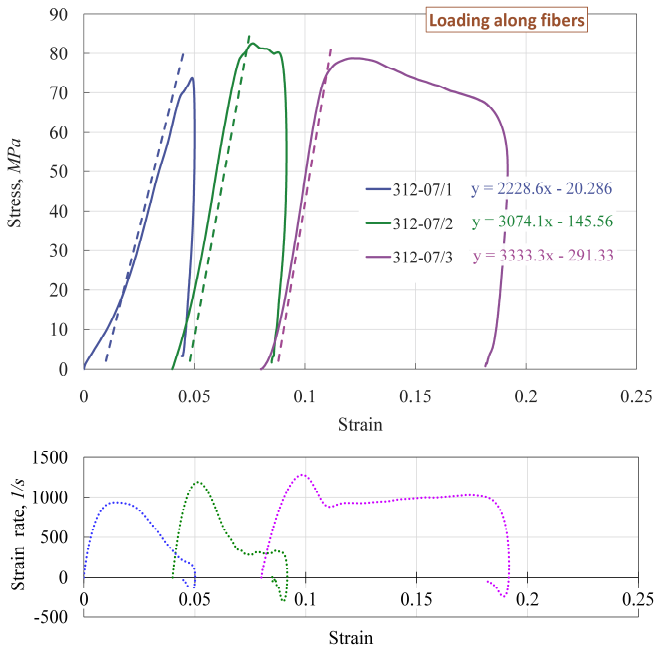

Fig. 3. Strain pulses in measuring bars

Fig. 4. Re-loading of sample 312-07 along the fibers
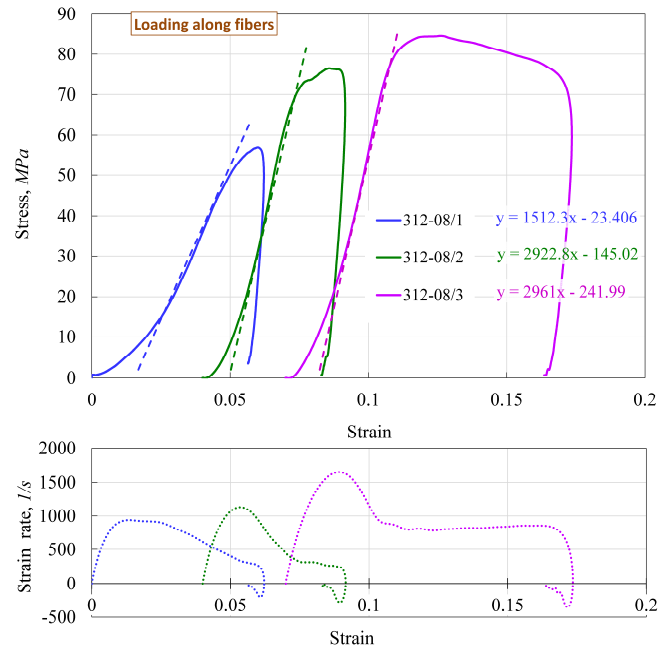

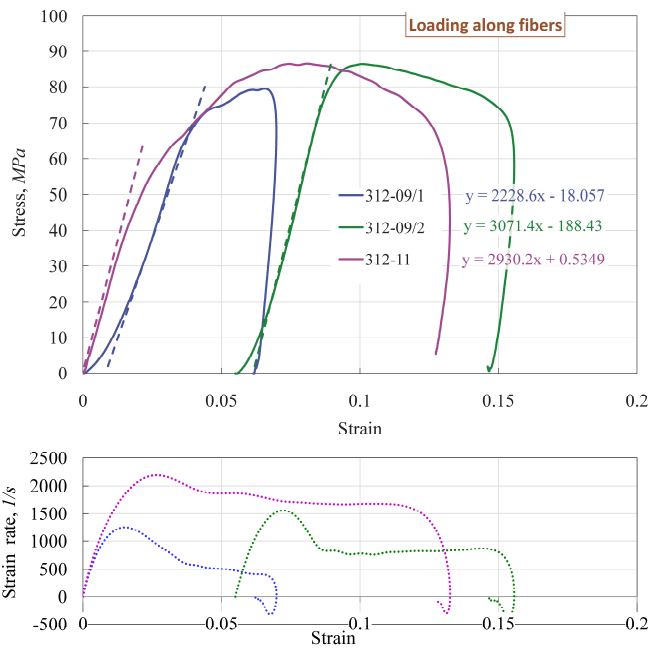**Fig. 5.** Re-loading sample 312-08 along the fibers

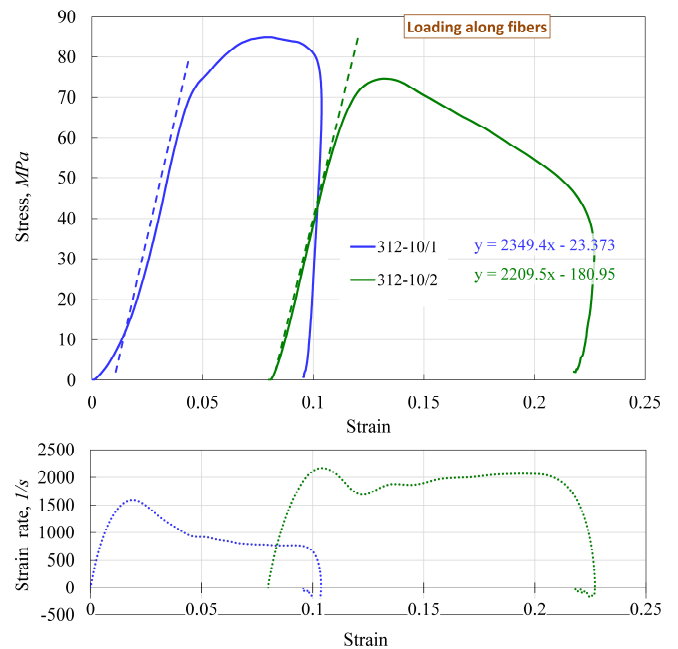**Fig. 6.** Loading of 312-09 and 312-11 samples along the fibers

Fig. 7. Double loading of sample 312-10 along the fibers

Figure 5 shows the results of triple loading of sample 312-08 with a strain rate increasing from experiment to experiment. As it can be seen in table 1, the strain degree of the sample in the first two loading cycles is insignificant, while in the third cycle the sample exhibits failure: the crack formation on its the side surface and its breaking into pieces.

From the obtained curves $\sigma_s(\varepsilon_s)$, the strain moduli of the sections of active loading were also determined. One can see the same tendency as in the previous sample: the deformation modulus increases under repeated loading.

Figure 6 shows double loading along the fibers of the sample 312-09 with the strain rate increasing from experiment to experiment (preserving the integrity of the sample after the first loading cycle), as well as a single loading of the sample 312-11 at a high loading velocity and failure. Significantly less nonlinearity of the initial section of the loading branch is noticeable. After testing, the sample had several longitudinal cracks, but after the end of the loading pulse effect, elastic unloading of the sample was seen to occur. The presence of elastic unloading of the sample indicates that when the wood is subjected to compression along the fibers, fracture of relatively weak bonds between them occurs, the fibers themselves being slightly compressed along and crooked followed by straightening after the end of the loading.
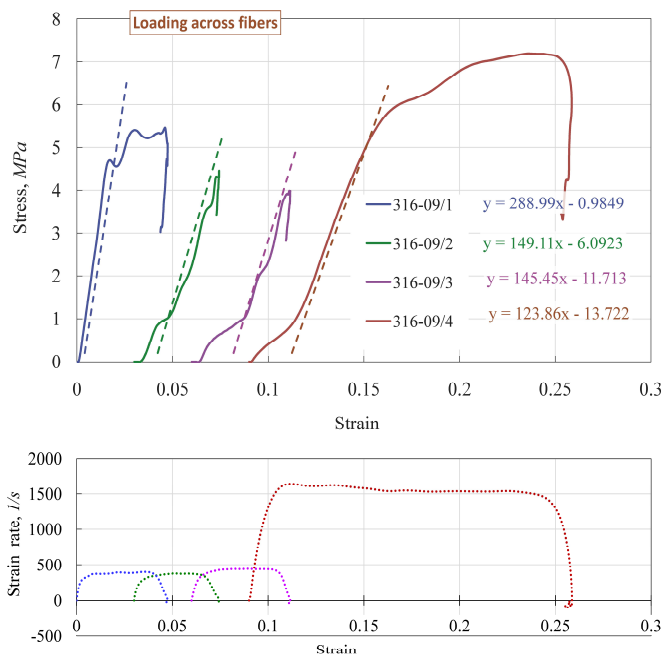
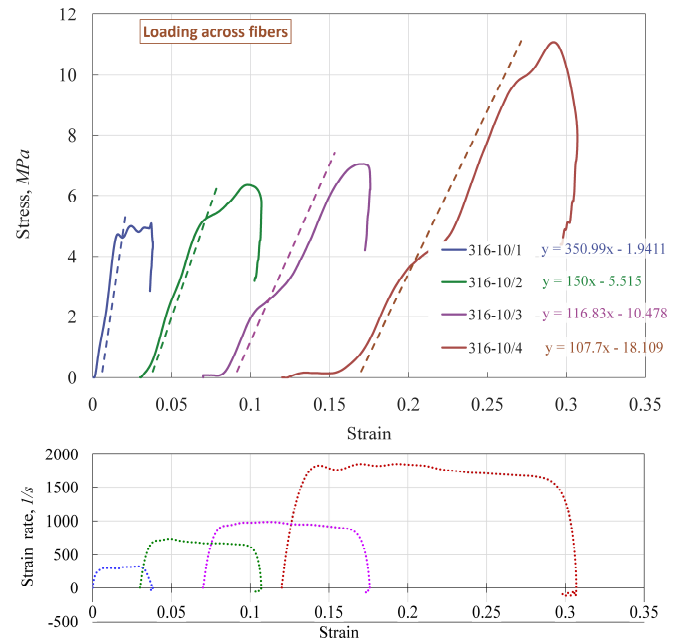**Fig. 8.** Fourfold loading of sample 316-09 across the fibers

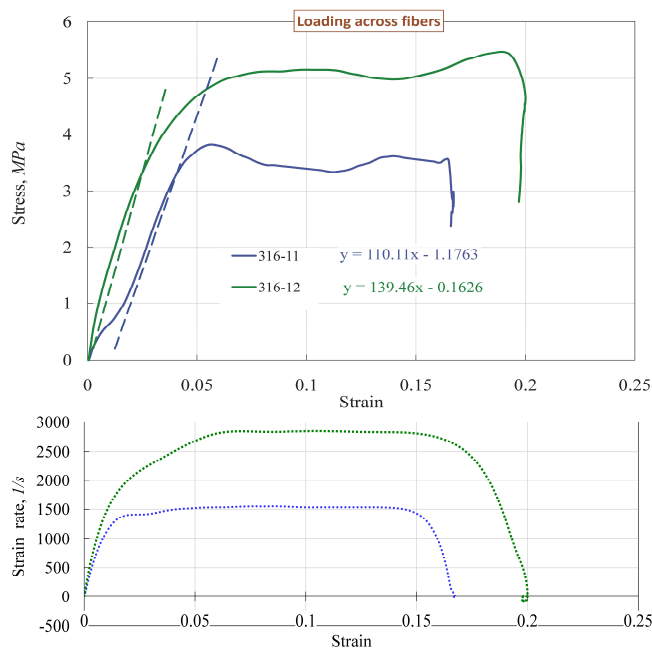**Fig. 9.** Fourfold loading of sample 316-10 across the fibers

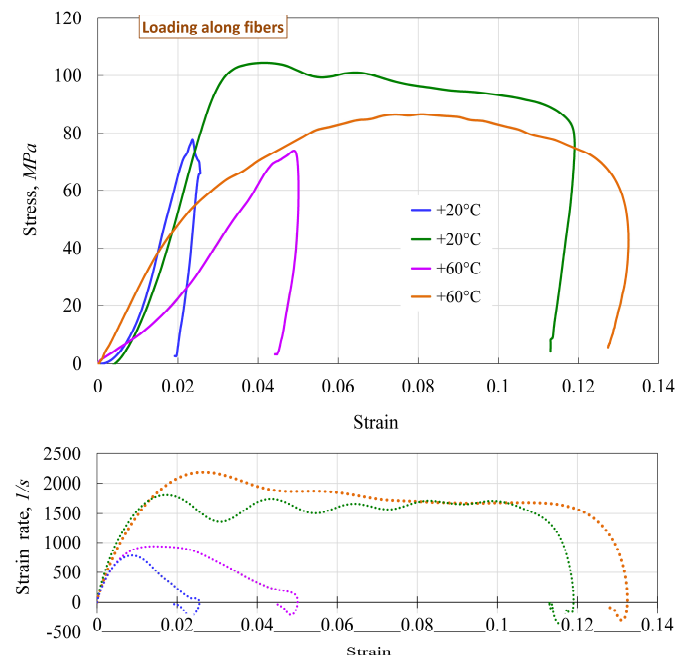**Fig. 10.** Loading samples 316-11 and 316-12 across the fibers

Fig. 11. The effect of temperature on the behavior of aspen samples along the fibers

The figure also shows an increase in the deformation modulus $d\sigma / d\varepsilon$ under repeated loading of sample 312-09. The dashed lines show the linear approximations of regions of active loading with corresponding equations. Under single loading with a high strain rate, the deformation modulus turned out to be larger than during the first loading.

Figure 7 shows double loading diagrams of sample 312-10. Moreover, in the first load cycle, the sample acquired a residual strain of 7.4%, although no external damage was noticed. The second loading cycle with a high strain rate did not lead to an increase in the achieved stresses and an increase in the deformation modulus. Apparently, during the first loading, serious internal damage occurred in the sample and its bearing capacity decreased.

Samples with a transverse arrangement of fibers were also loaded several times to assess fatigue life of the material. The obtained curves $\sigma_s(\varepsilon_s)$ and the corresponding dependences of the strain rate $\dot{\varepsilon}_s(\varepsilon_s)$ are shown in Figs. 8-10. Due to the high viscosity of the wood (especially its interfiber connective tissues), the unloading of the sample after the end of the loading pulse has a long duration and cannot be traced to the end due to the insufficient length of the measuring bars. It should be noted that the amplitude of the transmitted pulse for aspen samples under loading across the fibers is very small (of the order of 1-2 mV). Therefore, the signals from the reference bar were subjected to preliminary amplification.
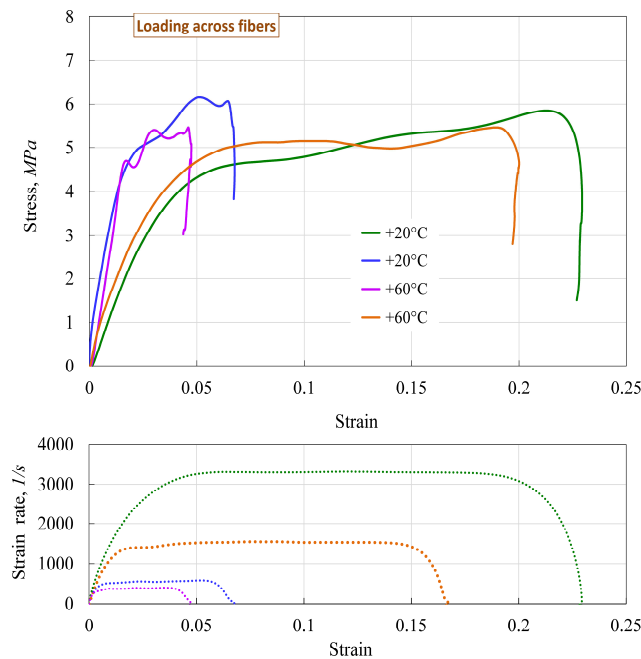
Fig. 12. The effect of temperature on the behavior of aspen samples across the fibers

Figure 8 shows a fourfold sequential loading of sample 316-09, and Fig. 9 presents the sample 316-10 under the same loading conditions. The test conditions obtained by the samples of residual deformations, as well as the strength and deformation characteristics determined by the diagrams, are shown in Table 1.

The diagrams shown in Figs. 8 and 9 indicate that there is a significant decrease in the linearity and steepness of the load branch during repeated loading cycles in samples with transverse fibers direction in contrast to those with longitudinal one. The stepped nature of the load branch is noticeable. Moreover, if the maximum stress during repeated loads with a similar strain rate becomes larger, then the magnitude of the step decreases.

Figure 10 shows the diagrams of two samples 316-11 and 316-12 under loading across the fibers with strain rates differing by a factor of 2. The strong effect of the strain rate on strength properties is seen. Modules of deformation of the active loading section differ by ~30%.

A comparison of the mechanical characteristics of aspen wood at elevated temperatures with similar characteristics obtained previously [8] at normal temperature is shown in Figs. 11 and 12. There is a good tendency toward a decrease in the deformation modulus of the area of active loading of samples along the fibers (Fig. 11). Strength properties at elevated temperatures are slightly reduced. It is difficult to give an unambiguous interpretation of the comparison of test results of samples across the fibers (Fig. 12) due to the difficulties of reliable registration of low-amplitude signals from the supporting bar and insufficient number of samples for a detailed study.

As can be seen from the above results, the properties of aspen wood at elevated temperatures up to +60°C differ from properties at room temperature. This should be taken into account when formulating a numerical model of wood.

5. Conclusion

According to the experimental results of aspen samples, the following general points in aspen behavior should be noted. For samples loaded along the fibers at strain rates above 1500 s^{-1}, on reaching the ultimate stress values, a decrease in stress (relaxation) is observed with strain increasing. The samples loaded across the fibers exhibit an almost horizontal region even with some hardening. Upon completion of the loading effect, despite significant sample damage, elastic unloading of the sample occurs with a significant residual deformation in it. Visual inspection of the samples after these experiments indicates their partial failure. Therefore, the maximum stress values can be taken as a characteristic of the material compressive strength. Comparison of the mechanical characteristics of aspen wood at elevated temperatures with similar characteristics at normal temperature showed that both the deformation modulus of the region of active loading along the fibers and strength properties decrease at elevated temperature. The obtained features of the behavior of aspen samples at elevated temperature should be taken into account when formulating a numerical model of wood.

Author Contributions

A. Bragov initiated the project and proposed a configuration of experiments; T. Yuzhina and A. Belov developed a program for processing and analyzing experimental information; A. Lomunov conducted dynamic experiments and analyzed empirical results; L. Igumnov checked the substantiation of the theory of deformation of anisotropic wood; V.A. Eremeyev planned and substantiated the experimental research scheme. The manuscript was written with the participation of all authors. All authors participated in the discussion of the results, and also reviewed and approved the final version of the manuscript.

Acknowledgments

Funding

Conflict of Interest

The authors declared no potential conflicts of interest concerning the research, authorship, and publication of this article.

Data Availability Statements

The datasets generated and/or analyzed during the current study are available from the corresponding author on reasonable request.

References

[1] Adalian, C., Morlier, P., "WOOD MODEL" for the dynamic behaviour of wood in multiaxial compression, *Holz als Roh- und Werkstoff,* 60, 2002, 433-439.
[2] Bragov, A., Gonov, M., Konstantinov, A., Lomunov, A., Yuzhina, T., Deformation and Destruction at Deformation Rate of Order 10^3 s^{-1} in Wood of Hardwood Trees, *Advanced Structured Materials*, 130, 2020, 443-451.
[3] Bragov, A.M., Lomunov, A.K., Methodological aspects of studying dynamic material properties using the Kolsky method, *International Journal of Impact Engineering*, 16(2), 1995, 321-330.
[4] Chen, W.W., Song, B., *Split Hopkinson (Kolsky) Bar. Design, Testing and Applications,* Springer US, 2010.
[5] Eisenacher, G., Scheidemann, R., Neumann, M., Wille, F., Droste, B., Crushing characteristics of spruce wood used in impact limiters of type B packages, *Proceedings of the 17th International Symposium on the Packaging and Transportation of Radioactive Materials PATRAM 2013*, August 18–23, San Francisco, USA. P. 1–10, 2013.
[6] Eisenacher, G., Wille, F., Droste, B., Neumann, M., Development of a wood material model for impact limiters of transport packages, *WM2014 Conference*, March 2-6, Phoenix, Arizona, USA, 1-10, 2014.
[7] Li, P., Guo, Y.B., Shim, V.P.W., A constitutive model for transversely isotropic material with anisotropic hardening, *International Journal of Solids and Structures*, 138, 2018, 40-49.
[8] Neumann, M., Herter, J., Droste, B.O., Hartwig, S., Compressive behaviour of axially loaded spruce wood under large deformations at different strain rates, *European Journal of Wood and Wood Products*, 69, 2011, 345-357.
[9] Tagarielli, V.L., Deshpande, V.S., Fleck, N.A., Chen, C., A constitutive model for transversely isotropic foams and its application to the indentation for balsa wood, *International Journal of Mechanical Sciences,* 47, 2005, 666-686.
[10] Zhao, S., Zhao, J.X., Han, G.Z., Advances in the study of mechanical properties and constitutive law in the field of wood research, *Materials Science and Engineering*, 137, 2016, 012036.

ORCID iD

Anatoly M. Bragov https://orcid.org/0000-0002-3122-2613
Tatyana N. Iuzhina https://orcid.org/0000-0001-6507-9547
Andrey K. Lomunov https://orcid.org/0000-0002-5966-2389
Leonid A. Igumnov https://orcid.org/0000-0003-3035-0119
Aleksandr A. Belov https://orcid.org/0000-0003-3704-048X
Victor A. Eremeev https://orcid.org/0000-0002-8128-3262

Publisher's Note Shahid Chamran University of Ahvaz remains neutral with regard to jurisdictional claims in published maps and institutional affiliations.